



ORIGINAL ARTICLE

Methylene Blue biodecolorization and biodegradation by immobilized mixed cultures of *Trichoderma viride* and *Ralstonia pickettii* into SA-PVA-Bentonite matrix



Badzlin Nabilah, Adi Setyo Purnomo *, Didik Prasetyoko, Alya Awinatul Rohmah

Department of Chemistry, Faculty of Science and Data Analytics, Institut Teknologi Sepuluh Nopember, ITS Sukolilo Campus, Surabaya, Indonesia

Received 21 November 2022; accepted 23 April 2023

Available online 28 April 2023

KEYWORDS

Methylene Blue;
Biodecolorization;
Ralstonia pickettii;
Trichoderma viride;
Immobilization;
Pollution

Abstract The problem of industrial dye wastewater poses a critical environmental challenge that demands urgent attention. This is because the direct release of synthetic dyes such as Methylene Blue (MB) into water bodies has been found to have adverse effects on the environment. Therefore, this study aimed to propose immobilization of a mixed *Trichoderma viride* and *Ralstonia pickettii* culture into Sodium alginate–Polyvinyl Alcohol–Bentonite (SA-PVA-Bentonite) matrix as a development method for MB decolorization and degradation. Immobilization process was carried out using the entrapment method, where bacteria and fungi cells were homogenized into the SA-PVA-Bentonite matrix. The results showed that immobilized culture (IMO Mix) outperformed the free cells in Mineral Salt Medium (MSM), achieving an impressive 97.88% decolorization rate for 48 h at 30 °C. Furthermore, a total of 3 metabolite product degradation were produced including Azure A and C, as well as Thionine by LCMS analysis. SEM-EDX analysis confirmed that culture was agglomerated within the SA-PVA-Bentonite matrix, while FTIR demonstrated the functional groups of the synthesized beads. Meanwhile, the difference in charge of bentonite facilitated the adsorption of MB onto the beads, and mixed culture supported the degradation process. This study presented a potential solution to environmental problems, particularly those related to

* Corresponding authors.

E-mail addresses: adi_setyo@chem.its.ac.id (A.S. Purnomo), didikp@chem.its.ac.id (D. Prasetyoko).

Peer review under responsibility of King Saud University.



the industrial sector. Further analysis was required to address the challenges associated with other industrial dye waste.

© 2023 The Author(s). Published by Elsevier B.V. on behalf of King Saud University. This is an open access article under the CC BY-NC-ND license (<http://creativecommons.org/licenses/by-nc-nd/4.0/>).

1. Introduction

Water is one of the most crucial components required for the sustenance of living organisms but human activities have led to a decline in the quality, primarily due to industrial activities (Bommavaram et al., 2020). The textile and paper industries are among the major contributors to water pollution, mainly due to their dyeing processes. About 15–30% of the dyes used during the manufacturing process result in wastewater and a decrease in water quality (Alkas et al., 2022; Tunç et al., 2009). Meanwhile, water bodies contaminated with high concentrations of synthetic dyes can lead to the mortality of aquatic organisms. The stable properties of dye wastewater are well-known to limit sunlight penetration, thereby reducing the rate of photosynthesis and causing a decline in the levels of dissolved oxygen (Lellis et al., 2019; Sharifi et al., 2022). The potential health risks associated with the intake of dye-contaminated water in high concentrations include allergies, cancer, and genetic mutations (Lellis et al., 2019).

MB is one of the cationic dyes commonly utilized in the textile and paper coloring industries, and the stable properties make it difficult to degrade naturally (Baguley et al., 2016; Moradi et al., 2021). Several methods such as adsorption, membrane filtration, photo-catalyst oxidation, Non-Thermal Plasma (NTP) catalysis, and coagulation have been developed for the dye waste treatment process (Ahmadzadeh et al., 2015; Dhiman et al., 2022; Liang et al., 2021; Robati et al., 2016). However, these methods are considered less effective due to the large residues produced during the process and the expensive reagent (Azam et al., 2020; Rizqi and Purnomo, 2017a). Adsorption is a simple and effective method that utilizes an adsorbent to remove dye and can degrade inorganic and organic compounds to become less toxic (Agarwal et al., 2016; Mahmood et al., 2022; Rajabi et al., 2016). Considering these factors, biodegradation is considered to be an efficient method for dye waste treatment as it is affordable and more environmentally friendly, utilizing bacteria or fungi to handle the waste (Cheng et al., 2012; Purnomo and Singh, 2017).

Fungi are one type of degrading agent more tolerant to pollutants than bacteria (Evans and Hedger, 2001). Furthermore, *Trichoderma viride* is a filamentous fungi with great potential in degrading pollutants. Lipsa et al. (2016) reported that *T. viride* can degrade polyester Poly-lactic Acid (PLA) and also adsorb heavy metal Pb(II) by forming a composite with Mica type phyllosilicate minerals such as muscovite, biotite, and phlogopite (Luo et al., 2021). This fungus showed great potential for MB biosorption by immobilizing within the Loofa sponge (Saeed et al., 2009). It produced a laccase enzyme that can degrade effluent dyes (Johnnie et al., 2021). Therefore, a modification of the development technique is required to effectively utilize these low-cost fungi agent.

The relationship between bacteria and fungi had been extensively studied since the 1960 s. Bacteria were reported to form a synergistic relationship with fungi in terms of wood decomposition process (Kamei et al., 2012). According to Clausen (1996), several metabolite products produced can increase the growth of fungi. The synergistic relationship increased the decolorization and degradation ability of MB by *T. viride*. Additionally, a bacteria used as a mixed culture with fungi is *Ralstonia pickettii*, due to its characteristics namely non-fermenting, gram-negative, aerobic, found in water and soil. It showed the ability to degrade aromatic compounds, such as benzene, cresol, phenol, and toluene (Ryan et al., 2007, 2006). Mahendra & Alvarez-Cohen (2006) reported that *R. pickettii* PK 01 degraded 50 mg/L 1,4 dioxane through a dioxane transformation process. In mixed culture, *R. pickettii* reportedly enhanced the ability of some fungi in the DDT degradation process (Purnomo et al., 2020, 2019).

The process of pollutant biodegradation can be carried out with the free cells method but has several shortcomings, such as the used cells being limited in operational stability, reusability, and transfer of substrates into the cells (Ha et al., 2009). Meanwhile, cell immobilization into a matrix is an effective technique for biodegradation, and entrapment is a technique used to trap cells in gels such as alginate, carrageenan, and Polyvinyl Alcohol (PVA) (Rodríguez Couto, 2009). Sodium Alginate (SA) is a natural polymer used in immobilization process due to its non-toxic and environmentally friendly properties. However, it has low mechanical durability and the beads are easily destroyed (de-Bashan and Bashan, 2010). To overcome this problem, SA can be mixed with PVA which has non-toxic and good durability properties (Bialik-Wąs et al., 2021). PVA is a synthetic polymer and has a good mechanical strength property. A review study showed that polymeric adsorbents have great applicability under different environmental conditions, such as dye toxic environments (Moradi and Sharma, 2021). Even though the combination of SA-PVA is extensively employed as an immobilization matrix, further refinement is necessary to augment its efficacy (Aljar et al., 2021).

Mineral clay is one of the materials currently attracting significant attention due to its low price, large abundance, and surface area, as well as good adsorption properties. In addition, several studies showed that it is effective in removing cationic dyes due to its negative charge (Aljar et al., 2021; Hosseini et al., 2021). Bentonite is a type of clay mineral that is composed of Si tetrahedral and Al octahedral interconnected layers of hydroxyl groups. Moreover, it is negatively charged and is neutralized by exchangeable cations (Hebbar et al., 2014). Oussalah & Boukerroui (2020) stated that bentonite has a strong affinity for MB dye, hence, the addition into the SA-PVA matrix can increase the adsorption ability and mechanical durability.

Based on the description above, this study was conducted to investigate the effect of *R. pickettii* and *T. viride* addition into the SA-PVA-Bentonite matrix on MB degradation and decolorization. Immobilization process improved its ability in MB decolorization process, by comparing within free cell treatment only. The study was also enhanced by the addition of bentonite that supported MB adsorption toward beads. Furthermore, *T. viride* and *R. pickettii* had the ability for degrading dye pollutants in sterile conditions, within 48 h of incubation time. Fourier Transform Infra-red (FTIR) and Scanning Electron Microscopy (SEM) characterizations were conducted to investigate the functional group and the morphological visual. Furthermore, the metabolite products that were produced and the biodegradation pathway used by immobilized mixed culture (IMO Mix) were also proposed.

2. Experimental

2.1. Materials

The materials used include filamentous fungi *T. viride* and bacterium *R. pickettii* obtained from Microorganism Chemistry Laboratory of Chemistry Department ITS, Potato Dextrose Agar (PDA, Himedia), Potato Dextrose Broth (PDB, Himedia), Nutrient Agar (NA, Merck), Luria Bertani Broth (LB, Merck), Aqua Demineralization (Aqua DM), 70% Alcohol (SAP Chemical), Bentonite, SA microbiology grade (Himedia), PVA with mass weight 60,000 (PVA, Merck), Glucose (Merck), NH_4NO_3 (SAP Chemical), K_2HPO_4 (SAP Chemical),

MgSO₄·7H₂O (SAP Chemical), KH₂PO₄ (SAP Chemical), and FeSO₄·7H₂O (SAP Chemical).

2.2. Culture condition

The bacterium culture of *R. pickettii* was inoculated on NA medium and incubated at 37 °C for 24 h. Meanwhile, the regenerated culture was taken with an ose needle and inoculated into 20 mL of LB medium. Bacteria inoculum was then activated in a shaker incubator for 24 h at 35 °C, and culture with OD 1 was placed into 180 mL of LB media. Subsequently, the bacterium culture was pre-incubated in a shaker incubator for 48 h at 35 °C (Sariwati et al., 2017; Wahyuni et al., 2017).

Culture of filamentous fungi *T. viride* was inoculated on PDA medium and incubated for 7 days at 30 °C (Pan et al., 2023). The regenerated fungus was then homogenized with 25 mL of sterile aqua DM. About 1 mL of the homogenate was inoculated into 9 mL of PDB medium, while the inoculum was pre-incubated for 7 days at 30 °C (Rizqi and Purnomo, 2017b).

2.3. Immobilization of mixed culture *T. viride* and *R. pickettii*

Immobilization process started with the synthesis of the SA-PVA-Bentonite matrix with a composition of 1:4:1 (%w/v), and the pre-incubated *T. viride* mycelium and *R. pickettii* cells were added to the hydrogel matrix, and homogenized. Furthermore, hydrogel IMO Mix was dropped into a 0.4 M CaCl₂ followed by constant stirring. The IMO Mix beads formed were immersed in a CaCl₂ solution for 24 h, and washed with sterile Aqua DM (Kurade et al., 2019; Oussalah and Boukerroui, 2020; Ramsay et al., 2005).

2.4. Beads characterization

The morphology of the beads produced was characterized through SEM-EDX characterization. Before the process, the beads were dried using a freeze dryer, and placed in the sample holder coated with gold powder (coating stage). Subsequently, the sample was placed into a vacuum chamber and analyzed using SEM.

FTIR characterization was carried out to identified the functional group of the SA-PVA-Bentonite and IMO Mix beads. FTIR analysis also obtained the functional groups on the IMO Mix beads before and after the decolorization process. Before the characterization process, the beads were dried using a freeze dryer and were ground with the addition of KBr. Furthermore, mixture was placed in a mold and hydraulically pressed to form a pellet in the sample holder for FTIR analysis.

2.5. MB biodecolorization test

IMO Mix beads were added into 100 mL of 50 mg/L MB solution in MSM + glucose medium. MB solution containing immobilized beads was then statically incubated for 48 h at 35 °C, pH 5.5. In addition, the decolorized solution was separated from the beads using the decantation method, and MB filtrate obtained was analyzed with the UV-Vis spectrophotometer. As a comparison, the decolorization process was also

performed by SA-PVA-Bentonite beads, free cells of *R. pickettii*, *T. viride*, and mix of them (FC RP, FC TV, and FC Mix, respectively), as well as immobilized cells of *R. pickettii* and *T. viride* (IMO RP and IMO TV, respectively). The calculation of MB removal percentage follows Equation (1), where [A]_k is the initial concentration and [A]_t is the final concentration of MB treatment.

$$MB \text{ Removal } (\%) = \frac{[A]_k - [A]_t}{[A]_k} \times 100\% \quad (1)$$

Some of the filtrate obtained from the decolorization process was also analyzed by Liquid Chromatography-Mass Spectroscopy (LCMS). The elution method used was the gradient with a flow rate of 0.2 mL/min and 0.4 mL/min in the first three and for the next seven minutes. The mobile phase employed was water and methanol with a ratio of 1:99 for the first three minutes and 39:66 for the remaining seven minutes. Additionally, the column used was an Acclaim TM RSLC 120 C18 type with a size of 2.1 × 100 mm and the temperature was 33 °C. In this study, the kinetics and isothermal adsorption of IMO Mix beads were also examined. The kinetic models used pseudo-first and pseudo-second order, while the adsorption kinetics were analyzed according to Langmuir and Freundlich isotherms.

3. Result and discussion

3.1. Mixed culture of *T. viride* and *R. pickettii* immobilization

Mixed culture of *T. viride* and *R. pickettii* was immobilized in the SA-PVA-Bentonite matrix for the biosorption and biodegradation processes. The two microbes produce enzymes needed in MB degradation process (Johnnie et al., 2021; Nabilah et al., 2022). In addition, immobilization process was carried out to increase the resistance of the bacterium and fungi to extreme environmental conditions, facilitate their separation from the degraded filtrate, and enable their reuse in multiple cycles (Dzionek et al., 2016; Partovinia and Rasekh, 2018). The entrapment method was an irreversible immobilization technique, where the microbes were trapped by a matrix or a hollow particle. This method was often used because it had a large immobilization capacity, a simple, inexpensive, and efficient diffusion process (Trelles and Rivero, 2013).

SA was one type of natural matrix used in immobilization process. This matrix was environmentally friendly and non-toxic or biocompatible, but had low mechanical strength (de-Bashan and Bashan, 2010). In this study, SA was mixed with PVA to increase its mechanical strength. A proper crosslinking agent was important to form a suitable beads matrix (Lu et al., 2022). In the SA-PVA hydrogel system, alginate formed cross-links with Ca²⁺ ions from CaCl₂, while PVA formed hydrogen bonds with alginate molecular chains (Hua et al., 2010). However, SA-PVA had been reported to have limitations in the decolorization process due to its low adsorption capacity and selectivity (Aljar et al., 2021). To solve this problem, bentonite was added to the SA-PVA matrix to increase the adsorption capacity. Bentonite is a type of negatively charged clay mineral neutralized in the presence of Na⁺ ions or K⁺ ions. These cations were bound to the silicate and could be easily replaced with others through an ion exchange process (Hebbar et al.,

2014). The presence of bentonite on matrix system was expected to increase the adsorption ability of MB dye.

Morphological structure and elemental analysis of the SA-PVA-Bentonite and IMO Mix beads were carried out by SEM-EDX. Before the characterization process, the beads were dried using a freeze-dryer, and the morphological structures are shown in Fig. 1. As indicated in Fig. 1a, SA-PVA-Bentonite beads have a hollow structure with slightly rough walls. This was similar to the results reported by Baigorria et al. (2020) and Xu et al. (2020), where the hollow structure provided more sites, potentially increasing the adsorption ability of the beads. The morphological structure of IMO Mix beads in Fig. 1b showed that there were many small cubes attached to the surface of the beads. Fouad et al. (2011) reported that the cubes represented the morphological structure of PVA. In addition, bentonite dispersed into the SA-PVA hydrogel, culminating in a relatively rough surface (Aljar et al., 2021). *T. viride* and *R. pickettii* added into matrix were not visible because their mycelia were well mixed during the homogenization process.

Table 2 showed the results of EDX analysis on SA-PVA-Bentonite and IMO Mix beads, where Fe and Mg elements were detected in bentonite structure (Hebbar et al., 2014). Additionally, elements K, S, P, and N were also detected on immobilized IMO Mix beads, indicating the presence of fungi and bacteria. Abostate et al. (2018) and Zylkiewicz et al. (2019) reported that EDX analysis of MAM bacteria and *Aspergillus* sp. showed some peaks of elements C, O, P, S, Cl, and K.

FTIR characterization was carried out to identify the functional groups formed on the beads. Fig. 2 provided clarification that SA-PVA-Bentonite and IMO Mix beads were constructed using SA, PVA, and bentonite. As evidenced in Fig. 2, the SA-PVA-Bentonite and IMO Mix synthesized before the bead formation exhibited a broad peak at $3,344\text{ cm}^{-1}$, indicating the overlapping-OH stretching of SA, PVA, and bentonite (Baigorria et al., 2020). Furthermore, the appearance of peaks at $1,624$, $1,423$, and $2,946\text{ cm}^{-1}$ represented asymmetric and symmetrical $-\text{COO}$ as well as $-\text{CH}$ stretching from alginate and PVA, respectively (Aljar et al., 2021). The shift of peaks at wave numbers $1,400\text{ cm}^{-1}$ was related to the presence of hydrogen bonds between the OH groups of PVA and alginate, or alginate and bentonite (Baigorria et al., 2020; Gonzalez et al., 2016). The SiO asymmetric and symmetrical from Si-O-Si of bentonite were represented by 1056 and 784 cm^{-1} (Baigorria et al., 2020; Belhouchat et al., 2017; Oussalah and Boukerroui, 2020). Therefore, it proved that IMO Mix and SA-PVA-Bentonite beads were consisted of SA, PVA, and bentonite.

A study showed that there was no significant difference observed in the FTIR analysis of *T. viride* before and after being loaded with MB (Saeed et al., 2009). The functional groups in the sample included OH, which overlapped with the amine functional group at 3368 cm^{-1} , as well as the carboxyl group and $-\text{NH}$ group, represented by peaks at 1654 and 1240 cm^{-1} , respectively. Additionally, FTIR analysis of bacteria provided information about the biomolecules present

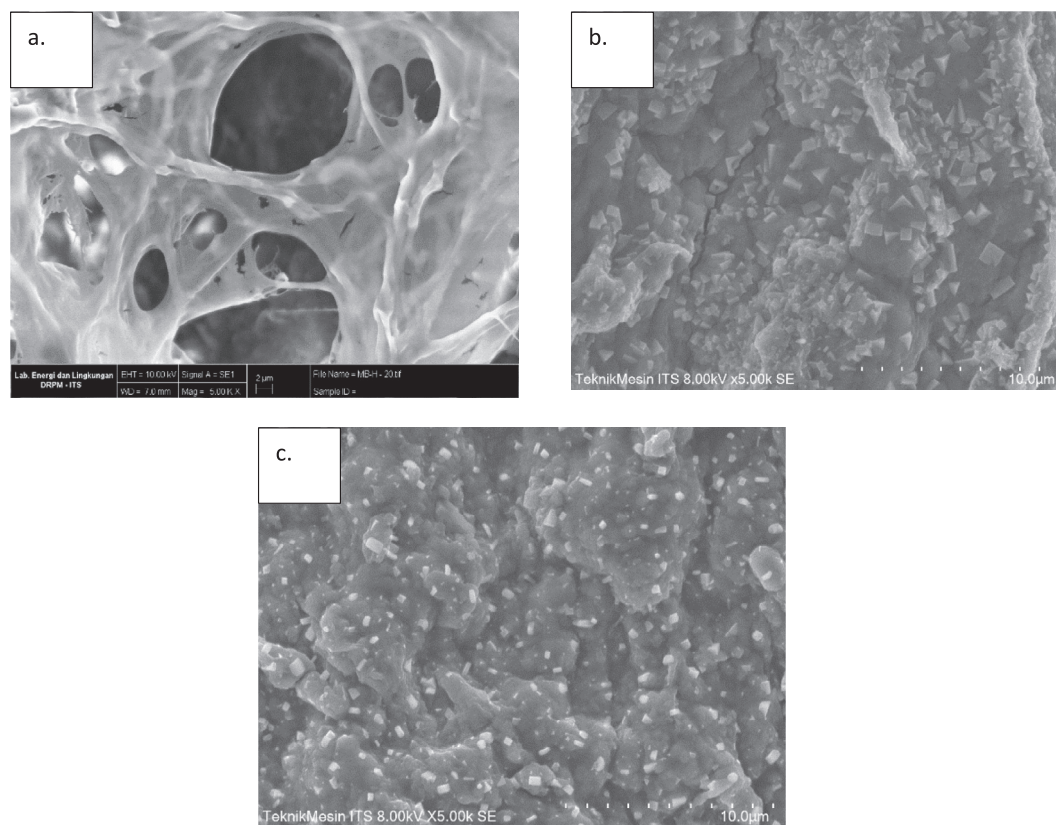


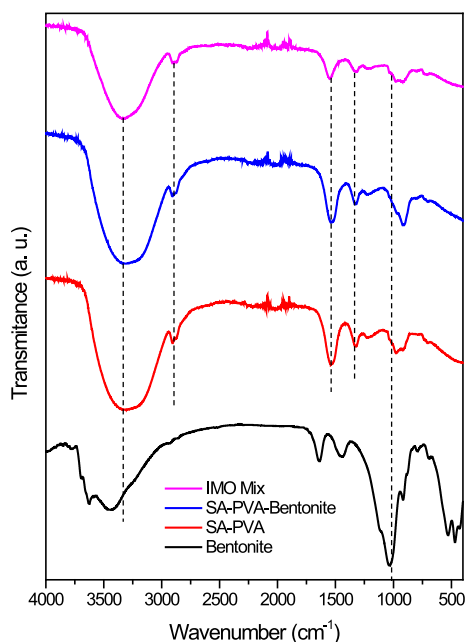
Fig. 1 Morphological structure of a) cross-section SA-PVA-B beads and b) immobilized mixed culture before decolorization c) immobilized mixed culture after decolorization.

Table 1 Calculation result of MB decolorization.

Sample	% Removal	Standard Deviation	Standard Error	Error Percentage (%)	Limit of Detection
FC RP	38.2	0.48	0.28	27.76%	8.26
IMO RP	96.81	0.42	0.24	24.49%	7.29
FC TV	69.49	0.07	0.04	4.08%	1.21
IMO TV	88.85	0.20	0.11	11.43%	3.40
FC Mix	94.6	0.07	0.04	4.08%	1.21
IMO Mix	97.88	0.11	0.07	6.53%	1.94
SA-PVA-Bentonite	78.98	0.27	0.16	15.51%	4.61

Table 2 EDX analysis of SA-PVA-Bentonite and IMO Mix beads.

Elements	Weight Percentage (Wt%)		
	SA-PVA-Bentonite	IMO Mix Before Decolorization	IMO Mix After Decolorization
O	54.26	36.78	35.73
C	33.65	0.83	1.65
Ca	6.20	18.76	14.70
Cl	5.28	18.78	6.20
Si	0.54	11.63	11.13
Al	0.08	5.12	5.05
Na		2.76	6.14
N		1.55	3.92
Mg		0.81	0.78
P		0.48	6.30
S		0.34	1.88
K		0.60	2.42
Fe		1.54	4.09

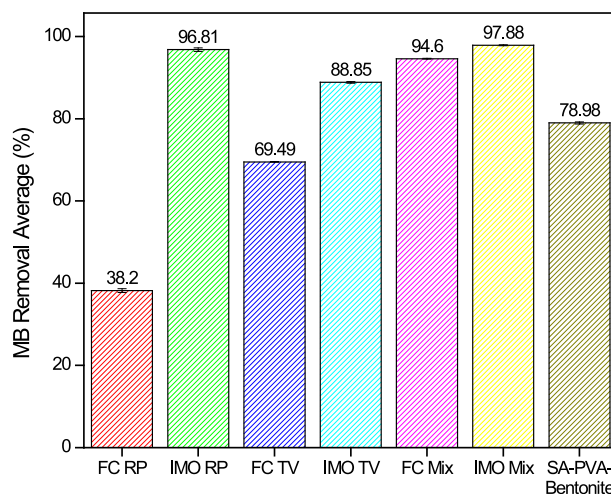
**Fig. 2** FTIR spectra.

in the sample. Naumann et al. (1991) classified five spectral windows due to the absorption expressed in lipid ($3000\text{--}2800\text{ cm}^{-1}$), protein and peptides ($1800\text{--}1500\text{ cm}^{-1}$), mixed region ($1500\text{--}1200\text{ cm}^{-1}$, for protein, fatty acid, and phosphate-carrying compounds), Polysaccharides ($1200\text{--}900\text{ cm}^{-1}$), and fingerprint region ($900\text{--}700\text{ cm}^{-1}$). Therefore, bacteria spectra showed OH, CH, amide, COO^- , C-O-C, and C-O (Novais et al., 2019).

3.2. MB biodecolorization

MB biodecolorization process by IMO Mix beads was performed by adding 40 g beads to 50 mg/L MB solution. The process was carried out in MSM with the addition of 0.5% (w/v) glucose. The medium used for the decolorization process was MSM, primarily due to its high mineral salt content, which is crucial for the growth and metabolism of microorganisms. Additionally, MSM is a low-carbon medium, resulting in the microorganisms being compelled to rely on supplementary carbon sources. The introduction of 0.5% glucose (w/v) into the medium served as a starter to facilitate the rapid acclimatization of the microorganisms to their new environment (Sekar and Mahadevan, 2011). MB biodecolorization process was conducted within 48 h, then the decolorized solution was measured with the UV-Vis spectrophotometer.

The comparison results of MB decolorization by IMO Mix beads and the other several decolorizing agents are shown in Fig. 3 within their analysis calculation that is shown at Table 1. The overall immobilized microorganisms in the SA-PVA-

**Fig. 3** MB removal percentage.

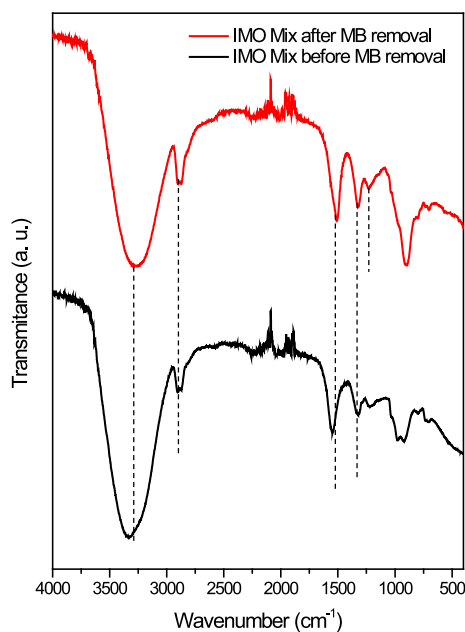


Fig. 4 FTIR spectra of immobilized mixed culture before and after decolorization.

Bentonite matrix caused a higher MB percent removal compared to the free cell due to the adsorption process mechanism by matrix. Additionally, the adsorption process occurred due to electrostatic interaction between the positive charge on the iminium group ($=N^+$) of MB and the negative charge ($-COO$, $-SiO^-$) in matrix (SA, PVA, and bentonite) (Aljar et al., 2021; Belhouchat et al., 2017; Zhang et al., 2021).

Fig. 3 showed that the presence of *R. pickettii* bacterium in mixed culture enhanced the ability of *T. viride* to decolorize MB. This was indicated by the increase in MB removal per-

centage with both free and immobilized cells. *R. pickettii* had been reported to enhance some ability of fungi in the pollutant degradation process. According to Nabilah et al. (2022), mixed culture decolorized MB up to 89%, while the use of *Daedalea dickinsii* independently caused only 17% decolorization. Based on Fig. 3, IMO Mix beads had the highest MB removal percentage of 97.88% among the samples tested. Even though the result did not show a significant difference with MB percentage removal of IMO RP, the metabolites product of mixed culture tends to be simpler. This was because the enzymes produced by mixed culture were more varied than the individual culture. Each culture in mixed sample would mutually degrade the intermediate compounds produced in the degradation process of the pollutant (Mawad et al., 2020; Zhang and Zhang, 2022).

MB was attracted by electrostatic interaction and hydrogen bonds toward the beads. The synthesized beads had a negatively charged condition due to the addition of bentonite (Ravi and Pandey, 2019). Bentonite exhibited an OH surface interaction and was capable of cation exchange, leading to its negatively charged state (Lin et al., 2014). Consequently, beads under the category of cationic dye, such as MB, interacted with the beads. In addition, the presence of SA, PVA, bentonite, and MB was supported by the occurrence of hydrogen bonds, as stated by Bialik-Was et al. (2021) and Ravi & Pandey (2019). The hydrogen bond arose from the interaction between electronegative atoms, such as F, O, N, and hydrogen.

MB biodecolorization process by IMO Mix was supported by SEM-EDX and FTIR characterization. Fig. 1c showed the morphological structure of IMO Mix beads after the decolorization process. Based on the results, immobilized beads after decolorization had a rougher morphological structure compared to before decolorization, as shown in Fig. 1b. This result was consistent with Ravi & Pandey (2019), where alginate-bentonite beads tend to have rougher morphological structures after MB adsorption process. EDX analysis results

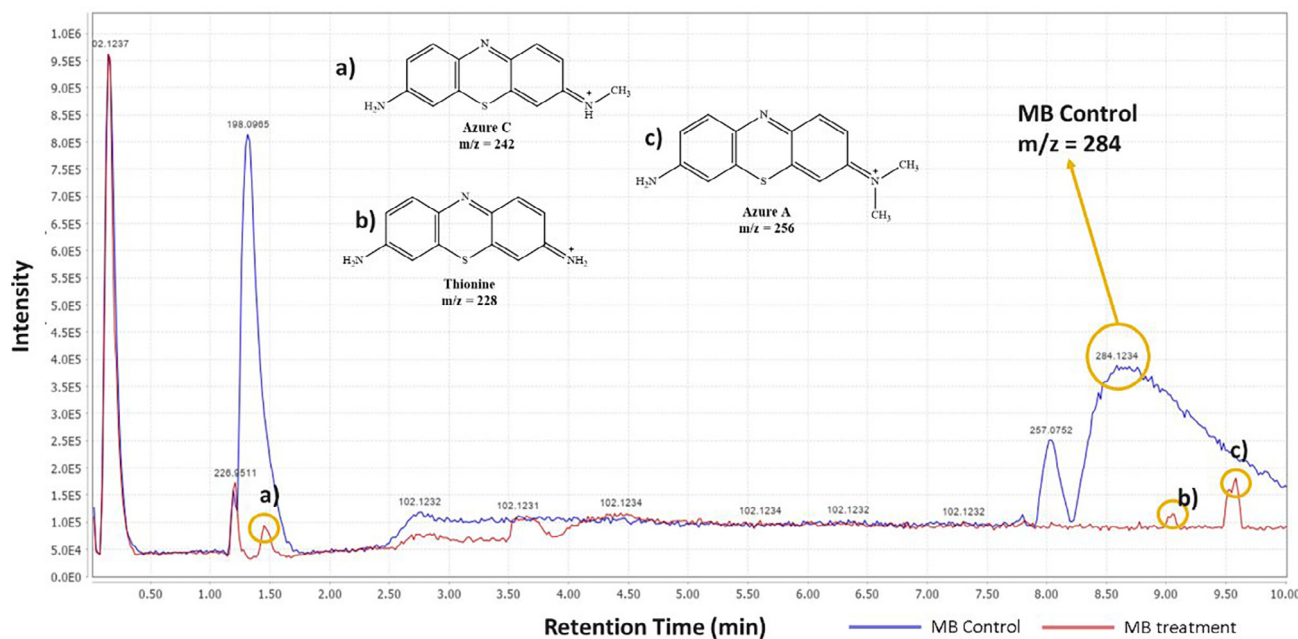


Fig. 5 The chromatogram comparison of MB control treatment.

of IMO Mix beads after decolorization are shown in Table 2, and the increase in the wt% of C, N, and S indicated the presence of MB adsorbed by immobilized beads. Meanwhile, the decrease in wt% of Ca implied the involvement of Ca^{2+} ions in the ion exchange process during MB adsorption.

Fig. 4 showed the FTIR spectra of IMO Mix beads before and after decolorization, the shifting peak of $-\text{OH}$ stretching from 3358 cm^{-1} to 3291 cm^{-1} on the beads after decolorization indicated the involvement of hydrogen bonds between bentonite in the beads and MB. A shift in the wave number of 1636 cm^{-1} to 1600 cm^{-1} indicated the presence of the $\text{C}=\text{C}$ group (Ravi and Pandey, 2019), while the appearance of a peak at 1332 cm^{-1} indicated the presence of C-N vibration of MB (Liu et al., 2020). These results supported the assumption that there was an interaction between the beads and MB.

3.3. Metabolite product identification

Metabolite products analysis of MB biodegradation product was carried out using LCMS. The instrument was a combination of HPLC and MS, where HPLC played a role in chromatographic separation and produces chromatograms, while MS provided m/z data of detected compounds (Winefordner, 2009). Fig. 5 showed the chromatogram comparison of MB treatment after decolorization and control (MB before decolorization).

MB peak was found at a retention time (t_R) of 8.50 in the treatment and control chromatogram. However, the intensity of peaks in the treatment chromatogram was significantly lower than in the control. This result proved the occurrence of MB degradation process by IMO Mix beads and also supported the previous analysis data by UV-Vis (Cohen et al., 2019). Fig. 5 showed that there were three new peaks in the treatment chromatogram at retention times of 1.47, 9.03, and 9.58, respectively. The three peaks obtained were identified as Azure C ($m/z = 242$), Thionine ($m/z = 228$), and Azure A ($m/z = 256$) (Hisaindee et al., 2013; Kishor et al., 2021; Rauf et al., 2010). In general, the product metabolites of MB biodegradation process are shown in Table 3.

The metabolites produced by several microorganisms showed different results depending on the enzymes released by the microbes. However, some microbes exhibited similar product metabolites. *Phanerochaete chrysosporium* and *Bacillus albus* MW507057 were also reported to degrade MB using the lignin peroxidase (LiP) enzyme through the demethylation reaction. The biodegradation by these two microorganisms produced Azure A and Thionine as metabolite products (Ferreira et al., 2000; Kishor et al., 2021). Based on the identification performed, MB degradation pathway by immobilized mixed culture of *T. viride* and *R. pickettii* involving the demethylase enzyme was proposed, as illustrated in Fig. 6. The degradation pathway began with oxidative demethylation from MB to Azure A and then to Azure C. Subsequently, Azure C was subjected to further demethylation reactions to produce product metabolites of Thionine (Ferreira et al., 2000; Kishor et al., 2021; Purnomo et al., 2010).

3.4. Adsorption kinetics and isotherms studies

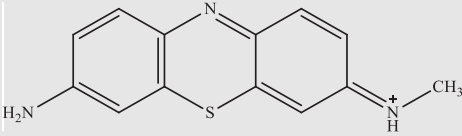
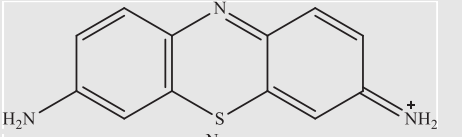
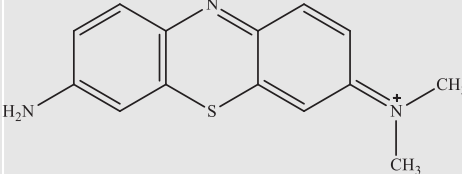
Adsorption kinetics should be analyzed to determine the adsorption rate and equilibrium capacity on the active site and surface area of the adsorbent (Das et al., 2021). In addition, this adsorption kinetics model depended on the physico-chemical conditions of the adsorbent. Kinetic studies explain how quickly contaminants were adsorbed on the surface of the adsorbent (Moradi and Daneshmand Sharabaf, 2022). In this study, two models of adsorption kinetics were used to evaluate the kinetics adsorption of IMO Mix beads. It was namely pseudo-first-order and pseudo-second order models which shown by Eq (2) and (3):

$$\ln(q_e - q_t) = \ln q_e - K_1 t \quad (2)$$

$$\frac{t}{q_t} = \frac{1}{K_2 q_e^2} + \frac{t}{q_e} \quad (3)$$

where q_t is the amount of adsorbate/dye adsorbed at time t (mg/g), q_e is the amount of adsorbate at equilibrium (mg/g), K_1 is the pseudo-first-order adsorption rate constant (min^{-1}),

Table 3 Product metabolites of MB biodegradation by IMO Mix beads.

Retention Time (t_R)	m/z	Metabolite Product	Molecular Structure
1.47	242	Azure C	
9.03	228	Thionine	
9.58	255	Azure A	

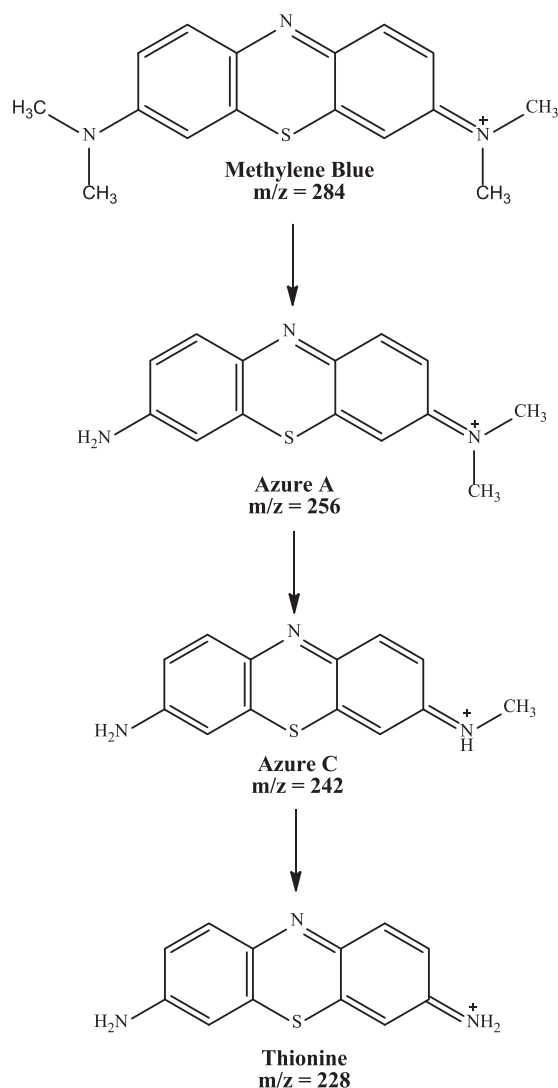


Fig. 6 Proposed MB degradation pathway by immobilized mixed culture of *T. viride* and *R. pickettii*.

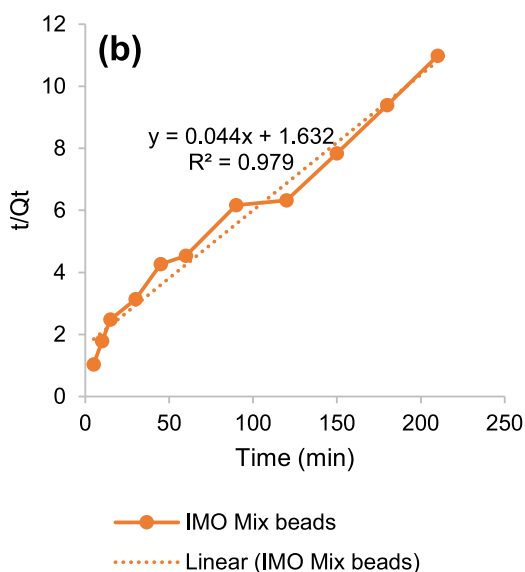
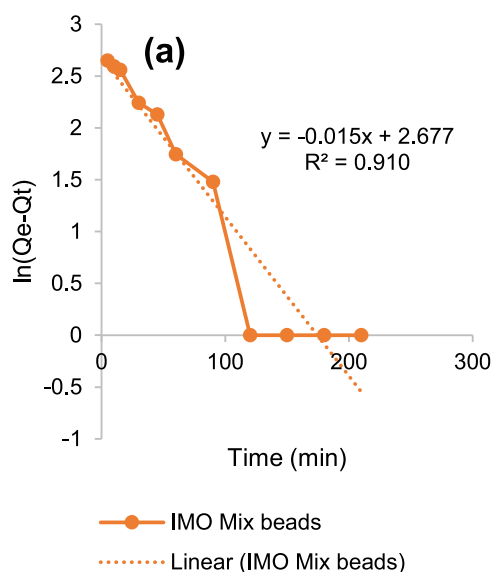


Fig. 7 Graphic of (a) pseudo-first and (b) pseudo-second order kinetic models.

and K_2 pseudo-second-order adsorption rate constant (g/mg min).

Correlation/regression coefficients value (R^2) close to 1 was obtained in pseudo-second order (Fig. 7). Meanwhile, R^2 of the pseudo-second-order was greater than the pseudo-first-order. Table 4 showed that the regression value and calculated q_e were determined to be 0.979 and 22.883 mg/g. The application of the pseudo-second-order kinetic model was based on the concept of chemisorption, where the rate of adsorption was dependent on the capacity (Das et al., 2021).

Adsorption isotherms showed the distribution of adsorbate molecules between the solid and liquid phases in solution at equilibrium. Furthermore, it indicated the amount of adsorption as a function of concentration at a constant temperature (Moradi et al., 2022), and the adsorption isotherms used Langmuir and Freundlich models. According to the Langmuir model, the distribution of the adsorbate was in the form of monolayer adsorption on the active site surface of the adsorbent. Meanwhile, the Freundlich model suggested that the adsorption occurred in multiple layers, known as multilayer adsorption (Freundlich and Heller, 1939; Langmuir, 1918). Langmuir and Freundlich model equations can be calculated by using the following equations (4) and (5), respectively:

$$\frac{1}{q_e} = \frac{1}{q_m} + \frac{1}{q_m K_L C_e} \quad (4)$$

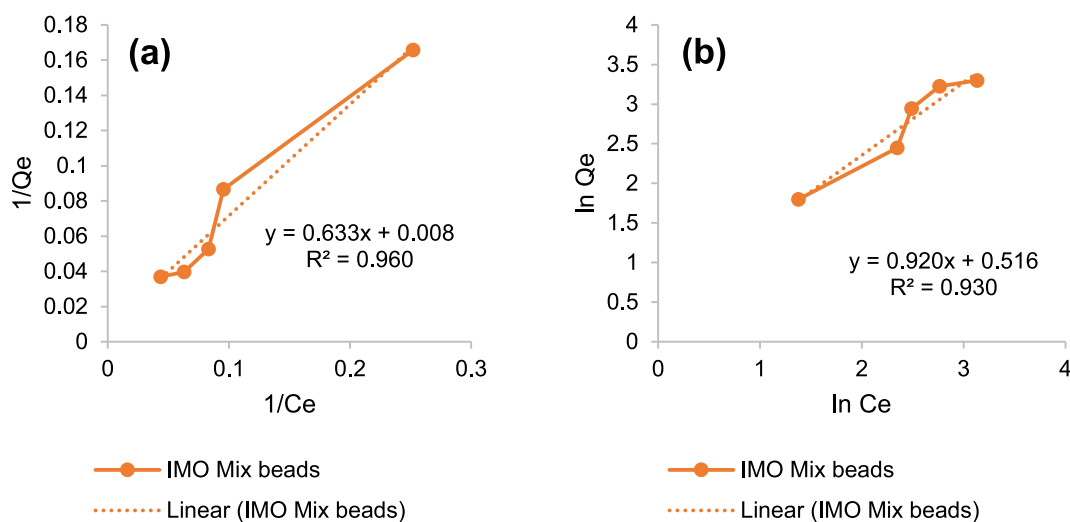
$$\ln q_e = \ln K_f + \frac{1}{n} \ln C_e \quad (5)$$

where q_e is the amount of adsorbate (mg/g), C_e is the concentration of adsorbate at equilibrium (mg/L), q_m is the maximum adsorption capacity (mg/g), K_L is the Langmuir adsorption constant (L/mg), and K_f is the Freundlich adsorption constant (L/mg).

Fig. 8 and Table 5 found that the R^2 of Langmuir isotherm value was close to 1 compared to Freundlich isotherm, and the regression was approximately 0.960. It showed the adsorption distribution of MB in IMO Mix beads occurred in monolayer adsorption. In addition, the maximum adsorption capacity of the beads was also obtained as 120.482 mg/g.

Table 4 Kinetic parameters of MB adsorption into IMO Mic beads.

Pseudo-first order					Pseudo-second order				
R ²	Slope	Intercept	K ₁	q _e cal	R ²	Slope	Intercept	K ₂	q _e cal
0.910	-0.015	2.677	0.015	0.985	0.979	0.044	1.632	0.001	22.883

**Fig. 8** Graphic of (a) Langmuir and (b) Freundlich adsorption isotherms.**Table 5** Isotherm adsorption of MB into IMO Mix.

Langmuir isotherm					Freundlich isotherm				
R ²	Slope	Intercept	K _L	q _m	R ²	Slope	Intercept	K _F	n
0.960	0.633	0.008	0.013	120.482	0.930	0.920	0.516	3.279	1.087

4. Conclusion

In conclusion, the synthesis of *T. viride* and *R. pickettii* mixed culture immobilized on the SA-PVA-Bentonite matrix (IMO Mix) was successfully performed. The beads produced were then used in MB biodecolorization and biodegradation processes. The results showed that IMO Mix beads decolorized MB up to 97.88% after 48 h incubation period. The metabolites that were produced from the biodegradation process consisted of Azure A and C, as well as Thionine. Those results showed a potential solution for MB removal and environment problem. Further analysis was required to test IMO Mix ability with other industrial dye waste.

Author contributions

BN and AAR investigated the experiment. ASP and DP conceptualized, supervised, and validated the experiment. BN, ASP, DP, and AAR wrote the original draft, as well as reviewed and edited the manuscript.

Declaration of Competing Interest

The authors declare that they have no known competing financial interests or personal relationships that could have appeared to influence the work reported in this paper.

Acknowledgments

The authors are grateful to the Directorate of Research, Technology, and Community Service, Ministry of Education, Culture, Research and Technology of Indonesia under the Student Thesis Research Scheme 2022, Number: 084/E5/PG.02.00. PT/2022 with Researcher Contract Number: 1434/PKS/ITS/2022, for funding this study.

References

- Abostate, M.A., Saleh, Y., Mira, H., Amin, M., Al, M., Ahmed, B.M., 2018. Characterization, kinetics and thermodynamics of biosynthesized uranium nanoparticles (UNPs). *Artif. Cells, Nanomed., Biotechnol.* 46, 147–159. <https://doi.org/10.1080/21691401.2017.1301460>.
- Agarwal, S., Tyagi, I., Gupta, V.K., Golbaz, F., Golikand, A.N., Moradi, O., 2016. Synthesis and characteristics of polyaniline/zirconium oxide conductive nanocomposite for dye adsorption application. *J. Mol. Liq.* 218, 494–498. <https://doi.org/10.1016/J.MOLLIQ.2016.02.040>.
- Ahmadzadeh, S., Rezayi, M., Kassim, A., Aghasi, M., 2015. Cesium selective polymeric membrane sensor based on p-isopropylcalix[6] arene and its application in environmental samples. *RSC Adv.* 5, 39209–39217. <https://doi.org/10.1039/c5ra02799c>.

- Aljar, M.A.A., Rashdan, S., El-fattah, A.A., 2021. Environmentally friendly Polyvi nyl alcohol – alginate / bentonite nanocomposite hydrogel beads as efficient adsorbents for removal of toxic Methylene Blue from aqueous solution. *Polymers (Basel)* 13, 4000. <https://doi.org/10.3390/polym13224000>.
- Alkas, T.R., Ediati, R., Ersam, T., Nawfa, R., Purnomo, A.S., 2022. Fabrication of metal-organic framework Universitas i Oslo-66 (UiO-66) and brown-rot fungus *Gloeophyllum trabeum* biocomposite (UiO-66 @ GT) and its application for reactive black 5 decolorization. *Arab. J. Chem.* 15,. <https://doi.org/10.1016/j.arabjc.2022.104129> 104129.
- Azam, K., Raza, R., Shezad, N., Shabir, M., Yang, W., Ahmad, N., Shafiq, I., Akhter, P., Razzaq, A., Hussain, M., 2020. Development of recoverable magnetic mesoporous carbon adsorbent for removal of methyl blue and methyl orange from wastewater. *J. Environ. Chem. Eng.* 8,. <https://doi.org/10.1016/j.jece.2020.104220> 104220.
- Baguley, B.C., Beland, C., Betz, J.M., Biggar, R.J., 2016. *Some Drugs and Herbal Product : IARC Monographs on The Evaluation of Carcinogenic Risks to Humans*. International Agency fro Research on Cancer, Lyon.
- Baigorria, E., Cano, L.A., Sanchez, L.M., Alvarez, V.A., Ollier, R.P., 2020. Bentonite-composite polyvinyl alcohol/alginate hydrogel beads: preparation, characterization and their use as arsenic removal devices. *Environ. Nanotechnol. Monit. Manag.* 14,. <https://doi.org/10.1016/j.enmm.2020.100364> 100364.
- Belhouchat, N., Zaghouane-Boudiaf, H., Viseras, C., 2017. Removal of anionic and cationic dyes from aqueous solution with activated organo-bentonite/sodium alginate encapsulated beads. *Appl. Clay Sci.* 135, 9–15. <https://doi.org/10.1016/j.clay.2016.08.031>.
- Bialik-Was, K., Królicka, E., Malina, D., 2021. Impact of the type of crosslinking agents on the properties of modified sodium alginate/poly(Vinyl alcohol) hydrogels. *Molecules* 26, 7–10. <https://doi.org/10.3390/molecules26082381>.
- Bommavaram, K., Yadav, A.B.D., Pandey, N.A.P., 2020. Tea residue as a bio - sorbent for the treatment of textile industry effluents. *Int. J. Environ. Sci. Technol.* 17, 3351–3364. <https://doi.org/10.1007/s13762-020-02628-w>.
- Cheng, Y., Lin, H.Y., Chen, Z., Megharaj, M., Naidu, R., 2012. Biodegradation of crystal violet using *Burkholderia vietnamiensis* C09V immobilized on PVA-sodium alginate-kaolin gel beads. *Ecotoxicol. Environ. Saf.* 83, 108–114. <https://doi.org/10.1016/j.ecoenv.2012.06.017>.
- Clausen, C.A., 1996. Bacterial associations with decaying wood: a review. *Int. Biodeterior. Biodegrad.* 37, 101–107. [https://doi.org/10.1016/0964-8305\(95\)00109-3](https://doi.org/10.1016/0964-8305(95)00109-3).
- Cohen, M., Ferroudj, N., Combes, A., Pichon, V., Abramson, S., 2019. Tracking the degradation pathway of three model aqueous pollutants in a heterogeneous Fenton process. *J. Environ. Chem. Eng.* 7,. <https://doi.org/10.1016/j.jece.2019.102987> 102987.
- Das, L., Saha, N., Ganguli, A., Das, P., Bhowal, A., Bhattacharjee, C., 2021. Calcium alginate–bentonite/activated biochar composite beads for removal of dye and Biodegradation of dye-loaded composite after use: synthesis, removal, mathematical modeling and biodegradation kinetics. *Environ. Technol. Innov.* 24,. <https://doi.org/10.1016/j.eti.2021.101955> 101955.
- de-Bashan, L.E., Bashan, Y., 2010. Immobilized microalgae for removing pollutants: Review of practical aspects. *Bioresour. Technol.* 101, 1611–1627. <https://doi.org/10.1016/j.biortech.2009.09.043>
- Dhiman, P., Goyal, D., Rana, G., Kumar, A., Sharma, G., Linxin, Kumar, G., 2022. Recent advances on carbon-based nanomaterials supported single-atom photo-catalysts for waste water remediation, *Journal of Nanostructure in Chemistry*. Springer Berlin Heidelberg. <https://doi.org/10.1007/s40097-022-00511-3>.
- Dzionek, A., Wojcieszynska, D., Guzik, U., 2016. Natural carriers in bioremediation: a review. *Electron. J. Biotechnol.* 23, 28–36. <https://doi.org/10.1016/j.ejbt.2016.07.003>.
- Evans, C.S., Hedger, J.N., 2001. *Degradation of Plant Cell Wall Polymers*. In: Gadd, G.M. (Ed.), *Fungi in Bioremediation*. Cambridge University Press, pp. 1–20.
- Ferreira, V.S., Magalhães, D.B., Kling, S.H., Da Silva Jr., J.G., Bon, E.P.S., 2000. N-Demethylation of Methylene Blue by Lignin Peroxidase from *Phanerochaete chrysosporium*. *Appl. Biochem. Biotechnol.* 84–86, 255–266. <https://doi.org/10.1385/ABAB:84-86:1-9:255>
- Fouad, E.A., El-badry, M., Mahrous, G.M., Alanazi, F.K., Neau, S. H., Alsarra, I.A., 2011. The use of spray-drying to enhance celecoxib solubility. *Drug Dev. Ind. Pharm.* 37, 1463–1472. <https://doi.org/10.3109/03639045.2011.587428>.
- Freundlich, H., Heller, W., 1939. The adsorption of cis-and trans-azobenzene. *J. Am. Chem. Soc.* 61, 2228–2230. <https://doi.org/10.1021/ja01877a071>.
- Gonzalez, J.S., Ponce, A., Alvarez, V.A., 2016. Preparation and characterization of poly (vinylalcohol) / bentonite hydrogels for potential wound dressings. *Adv. Mater. Lett.* 7, 100–150. <https://doi.org/10.5185/amlett.2016.6888>.
- Ha, J., Engler, C.R., Wild, J.R., 2009. Biodegradation of coumaphos, chlorferon, and diethylthiophosphate using bacteria immobilized in Ca-alginate gel beads. *Bioresour. Technol.* 100, 1138–1142. <https://doi.org/10.1016/j.biortech.2008.08.022>.
- Hebbar, R.S., Isloor, A.M., Ismail, A.F., 2014. Preparation and evaluation of heavy metal rejection properties of polyetherimide/porous activated bentonite clay nanocomposite membrane. *RSC Adv.* 4, 47240–47248. <https://doi.org/10.1039/C4RA09018G>.
- Hisaidee, S., Meetani, M.A., Rauf, M.A., 2013. Application of LC-MS to the analysis of advanced oxidation process (AOP) degradation of dye products and reaction mechanisms. *Trends Anal. Chem.* 49, 31–44. <https://doi.org/10.1016/j.trac.2013.03.011>.
- Hosseini, S.A., Daneshvar, S., Vossoughi, M., Simchi, A., Sadrzadeh, M., 2021. Green electrospun membranes based on chitosan / amino- functionalized nanoclay composite fibers for cationic dye removal : synthesis and kinetic studies. *ACS Omega* 6, 10816–10827. <https://doi.org/10.1021/acsomega.1c00480>.
- Hua, S., Ma, H., Li, X., Yang, H., Wang, A., 2010. pH-sensitive sodium alginate/poly(vinyl alcohol) hydrogel beads prepared by combined Ca²⁺ crosslinking and freeze-thawing cycles for controlled release of diclofenac sodium. *Int. J. Biol. Macromol.* 46, 517–523. <https://doi.org/10.1016/j.ijbiomac.2010.03.004>.
- Johnnie, D.A., Issac, R., Prabha, M.L., 2021. Bio efficacy assay of laccase isolated and characterized from *trichoderma viride* in biodegradation of low density polyethylene (LDPE) and textile industrial effluent dyes. *J. Pure Appl. Microbiol.* 15, 410–420. <https://doi.org/10.22207/JPAM.15.1.38>.
- Kamei, I., Yoshida, T., Enami, D., Meguro, S., 2012. Coexisting *Curtobacterium* bacterium promotes growth of white-rot fungus *Stereum* sp. *Curr. Microbiol.* 64, 173–178. <https://doi.org/10.1007/s00284-011-0050-y>.
- Kishor, R., Saratale, G.D., Saratale, R.G., Romanholo Ferreira, L.F., Bilal, M., Iqbal, H.M.N., Bharagava, R.N., 2021. Efficient degradation and detoxification of methylene blue dye by a newly isolated ligninolytic enzyme producing bacterium *Bacillus albus* MW407057. *Colloids Surf. B Biointerfaces* 206,. <https://doi.org/10.1016/j.colsurf.2021.111947> 111947.
- Kurade, M.B., Waghmode, T.R., Xiong, J.Q., Govindwar, S.P., Jeon, B.H., 2019. Decolorization of textile industry effluent using immobilized consortium cells in upflow fixed bed reactor. *J. Clean. Prod.* 213, 884–891. <https://doi.org/10.1016/j.jclepro.2018.12.218>.
- Langmuir, I., 1918. The adsorption of gases on plane surfaces of glass, mica and platinum. *J. Am. Chem. Soc.* 40, 1361–1403. <https://doi.org/10.1021/ja02242a004>.
- Lellis, B., Fávoro-Polonio, C.Z., Pamphile, J.A., Polonio, J.C., 2019. Effects of textile dyes on health and the environment and bioremediation potential of living organisms. *Biotechnol. Res. Innov.* 3, 275–290. <https://doi.org/10.1016/j.biori.2019.09.001>.

- Liang, Y., Li, J., Xue, Y., Tan, T., Jiang, Z., He, Y., Shanguan, W., Yang, J., Pan, Y., 2021. Benzene decomposition by non-thermal plasma: a detailed mechanism study by synchrotron radiation photoionization mass spectrometry and theoretical calculations. *J. Hazard. Mater.* 420,. <https://doi.org/10.1016/j.jhazmat.2021.126584> 126584.
- Lin, C., Gan, L., Chen, Z., Megharaj, M., Naidu, R., 2014. Biodegradation of naphthalene using a functional biomaterial based on immobilized *Bacillus fusiformis* (BFN). *Biochem. Eng. J.* 90, 1–7. <https://doi.org/10.1016/j.bej.2014.05.003>.
- Lipsa, R., Tudorachi, N., Darie-Nita, R.N., Oprică, L., Vasile, C., Chiriac, A., 2016. Biodegradation of poly(lactic acid) and some of its based systems with *Trichoderma viride*. *Int. J. Biol. Macromol.* 88, 515–526. <https://doi.org/10.1016/j.ijbiomac.2016.04.017>.
- Liu, Y., Zhao, Y., Cheng, W., Zhang, T., 2020. Targeted reclaiming cationic dyes from dyeing wastewater with a dithiocarbamate-functionalized material through selective adsorption and efficient desorption. *J. Colloid Interface Sci.* 579, 766–777. <https://doi.org/10.1016/j.jcis.2020.06.083>.
- Lu, J., Chen, Y.i., Ding, M., Fan, X., Hu, J., Chen, Y., Li, J., Li, Z., Liu, W., 2022. A 4arm-PEG macromolecule crosslinked chitosan hydrogels as antibacterial wound dressing. *Carbohydr. Polym.* 277,. <https://doi.org/10.1016/j.carbpol.2021.118871> 118871.
- Luo, D., Geng, R., Wang, W., Ding, Z., Qiang, S., Liang, J., Li, P., Zhang, Y., Fan, Q., 2021. *Trichoderma viride* involvement in the sorption of Pb(II) on muscovite, biotite and phlogopite: batch and spectroscopic studies. *J. Hazard. Mater.* 401,. <https://doi.org/10.1016/j.jhazmat.2020.123249> 123249.
- Mahendra, S., Alvarez-Cohen, L., 2006. Kinetics of 1,4-dioxane biodegradation by monooxygenase-expressing bacteria. *Environ. Sci. Technol.* 40, 5435–5442. <https://doi.org/10.1021/es060714v>.
- Mahmood, K., Amara, U., Siddique, S., Usman, M., Peng, Q., Khalid, M., Hussain, A., Ajmal, M., Ahmad, A., Sumrra, S.H., Liu, Z.-P., Khan, W.S., Ashiq, M.N., 2022. Green synthesis of Ag@CdO nanocomposite and their application towards brilliant green dye degradation from wastewater. *J. Nanostruct. Chem.* 12, 329–341. <https://doi.org/10.1007/s40097-021-00418-5>.
- Mawad, A.M.M., El-Latif Hesham, A., Yousef, N.M.H., Shoreit, A. A.M., Gathergood, N., Gupta, V.K., 2020. Role of bacterial-fungal consortium for enhancement in the degradation of industrial dyes. *Curr. Genomics* 21, 283–294. <https://doi.org/10.2174/1389202921999200505082901>.
- Moradi, O., Daneshmand Sharabaf, I., 2022. Separation of organic contaminant (dye) using the modified porous metal-organic framework (MIL). *Environ. Res.* 214. <https://doi.org/10.1016/j.envres.2022.114006>.
- Moradi, O., Sharma, G., 2021. Emerging novel polymeric adsorbents for removing dyes from wastewater: a comprehensive review and comparison with other adsorbents. *Environ. Res.* 201,. <https://doi.org/10.1016/J.ENVIRES.2021.111534> 111534.
- Moradi, O., Madanpisheh, M.A., Moghaddas, M., 2021. Synthesis of GO/HEMA, GO/HEMA/TiO₂, and GO/Fe₃O₄/HEMA as novel nanocomposites and their dye removal ability. *Adv. Compos. Hybrid Mater.* 4, 1185–1204. <https://doi.org/10.1007/s42114-021-00353-7>.
- Moradi, O., Pudineh, A., Sedaghat, S., 2022. Synthesis and characterization Agar/GO/ZnO NPs nanocomposite for removal of methylene blue and methyl orange as azo dyes from food industrial effluents. *Food Chem. Toxicol.* 169,. <https://doi.org/10.1016/j.fct.2022.113412> 113412.
- Nabilah, B., Purnomo, A.S., Rizqi, H.D., Putro, H.S., Nawfa, R., 2022. The effect of *Ralstonia pickettii* bacterium addition on methylene blue dye biodecolorization by brown-rot fungus *Daedalea dickinsii*. *Heliyon* 8, e08963. <https://doi.org/10.1016/J.HELIYON.2022.E08963>.
- Naumann, D., Helm, D., Labischinski, H., 1991. Microbiological characterizations by FT-IR spectroscopy. *Nature* 351, 81–82. <https://doi.org/10.1038/351081a0>.
- Novais, Â., Freitas, A.R., Rodrigues, C., Peixe, L., 2019. Fourier transform infrared spectroscopy: unlocking fundamentals and prospects for bacterial strain typing. *Eur. J. Clin. Microbiol. Infect. Dis.* 38, 427–448. <https://doi.org/10.1007/s10096-018-3431-3>.
- Oussalah, A., Boukerroui, A., 2020. Alginate-bentonite beads for efficient adsorption of Methylene Blue dye. *Euro-Mediterranean J. Environ. Integr.* 5, 31. <https://doi.org/10.1007/s41207-020-00165-z>.
- Pan, C., Yang, K., Erhunmwunsee, F., Li, Y.X., Liu, M., Pan, S., Yang, D., Lu, G., Ma, D., Tian, J., 2023. Inhibitory effect of cinnamaldehyde on *Fusarium solani* and its application in postharvest preservation of sweet potato. *Food Chem.* 408,. <https://doi.org/10.1016/j.foodchem.2022.135213> 135213.
- Partovinia, A., Rasekh, B., 2018. Review of the immobilized microbial cell systems for bioremediation of petroleum hydrocarbons polluted environments. *Crit. Rev. Environ. Sci. Technol.* 48, 1–38. <https://doi.org/10.1080/10643389.2018.1439652>.
- Purnomo, A.S., 2017. Microbe-Assisted Degradation of Aldrin and Dieldrin. In: Singh, S. (Ed.), *Microbe-Induced Degradation of Pesticides*. *Environ. Eng. Sci.* Springer, Cham. https://doi.org/10.1007/978-3-319-45156-5_1.
- Purnomo, A.S., Mori, T., Kondo, R., 2010. Involvement of Fenton reaction in DDT degradation by brown-rot fungi. *Int. Biodeterior. Biodegrad.* 64, 560–565. <https://doi.org/10.1016/j.ibiod.2010.06.008>.
- Purnomo, A.S., Maulianawati, D., Kamei, I., 2019. *Ralstonia pickettii* enhance the DDT biodegradation by *Pleurotus eryngii*. *J. Microbiol. Biotechnol.* 29, 1424–1433. <https://doi.org/10.4014/jmb.1906.06030>.
- Purnomo, A.S., Sariwati, A., Kamei, I., 2020. Synergistic interaction of a Consortium of the brown-rot fungus *Fomitopsis pinicola* and the Bacterium *Ralstonia pickettii* for DDT biodegradation. *Heliyon* 6, e04027. <https://doi.org/10.1016/j.heliyon.2020.e04027>.
- Rajabi, M., Mirza, B., Mahanpoor, K., Mirjalili, M., Najafi, F., Moradi, O., Sadegh, H., Shahryari-ghoshekandi, R., Asif, M., Tyagi, I., Agarwal, S., Gupta, V.K., 2016. Adsorption of malachite green from aqueous solution by carboxylate group functionalized multi-walled carbon nanotubes: determination of equilibrium and kinetics parameters. *J. Ind. Eng. Chem.* 34, 130–138. <https://doi.org/10.1016/J.JIEC.2015.11.001>.
- Ramsay, J.A., Mok, W.H.W., Luu, Y.S., Savage, M., 2005. Decoloration of textile dyes by alginate-immobilized *Trametes versicolor*. *Chemosphere* 61, 956–964. <https://doi.org/10.1016/j.chemosphere.2005.03.070>.
- Rauf, M.A., Meetani, M.A., Khaleel, A., Ahmed, A., 2010. Photocatalytic degradation of Methylene Blue using a mixed catalyst and product analysis by LC/MS. *Chem. Eng. J.* 157, 373–378. <https://doi.org/10.1016/j.cej.2009.11.017>.
- Ravi, Pandey, L.M., 2019. Enhanced adsorption capacity of designed bentonite and alginate beads for the effective removal of methylene blue. *Appl. Clay Sci.* 169, 102–111. <https://doi.org/10.1016/j.clay.2018.12.019>.
- Rizqi, H.D., Purnomo, A.S., 2017a. The ability of brown-rot fungus *Daedalea dickinsii* to decolorize and transform Methylene Blue dye. *World J. Microbiol. Biotechnol.* 33, 92. <https://doi.org/10.1007/s11274-017-2256-z>.
- Rizqi, H.D., Purnomo, A.S., 2017b. The ability of brown-rot fungus *Daedalea dickinsii* to decolorize and transform methylene blue dye. *World J. Microbiol. Biotechnol.* 33, 1–9. <https://doi.org/10.1007/s11274-017-2256-z>.
- Robati, D., Mirza, B., Rajabi, M., Moradi, O., Tyagi, I., Agarwal, S., Gupta, V.K., 2016. Removal of hazardous dyes-BR 12 and methyl orange using graphene oxide as an adsorbent from aqueous phase. *Chem. Eng. J.* 284, 687–697. <https://doi.org/10.1016/J.CEJ.2015.08.131>.
- Rodríguez Couto, S., 2009. Dye removal by immobilised fungi. *Biotechnol. Adv.* 27, 227–235. <https://doi.org/10.1016/j.biotechadv.2008.12.001>.

- Ryan, M.P., Pembroke, J.T., Adley, C.C., 2006. *Ralstonia pickettii*: a persistent gram-negative nosocomial infectious organism. *J. Hosp. Infect.* 62, 278–284. <https://doi.org/10.1016/j.jhin.2005.08.015>.
- Ryan, M.P., Pembroke, J.T., Adley, C.C., 2007. *Ralstonia pickettii* in environmental biotechnology: potential and applications. *J. Appl. Microbiol.* 103, 754–764. <https://doi.org/10.1111/j.1365-2672.2007.03361.x>.
- Saeed, A., Iqbal, M., Zafar, S.I., 2009. Immobilization of *Trichoderma viride* for enhanced methylene blue biosorption: batch and column studies. *J. Hazard. Mater.* 168, 406–415. <https://doi.org/10.1016/j.jhazmat.2009.02.058>.
- Sariwati, A., Purnomo, A.S., Kamei, I., 2017. Abilities of Co-cultures of brown-rot fungus *Fomitopsis pinicola* and *Bacillus subtilis* on biodegradation of DDT. *Curr. Microbiol.* 74, 1068–1075. <https://doi.org/10.1007/s00284-017-1286-y>.
- Sekar, S., Mahadevan, S., 2011. Thermokinetic responses of the metabolic activity of *Staphylococcus lentus* cultivated in a glucose limited mineral salt medium. *J. Therm. Anal. Calorim.* 104, 149–155. <https://doi.org/10.1007/s10973-010-1121-1>.
- Sharifi, M., Marjani, A., Mahdavian, L., Shamlouei, H.R., 2022. Density functional theory study of dyes removal from colored wastewater by a nano-composite of polysulfone/polyethylene glycol. *J. Nanostruct. Chem.* <https://doi.org/10.1007/s40097-022-00502-4>.
- Trelles, J.A., Rivero, C.W., 2013. In: *Whole Cell Entrapment Techniques BT - Immobilization of Enzymes and Cells*. Third Edition. Humana Press, Totowa, NJ, pp. 365–374. https://doi.org/10.1007/978-1-62703-550-7_24.
- Tunç, Ö., Tanaci, H., Aksu, Z., 2009. Potential use of cotton plant wastes for the removal of Remazol Black B reactive dye. *J. Hazard. Mater.* <https://doi.org/10.1016/j.jhazmat.2008.06.078>.
- Wahyuni, S., Khaeruni, A., Purnomo, A.S., Asranudin, Holilah, Fatahu, 2017. Characterization of mannanase isolated from corn-cob waste bacteria. *Asian J. Chem.* 29 (5), 1119–1120. <https://doi.org/10.14233/ajchem.2017.20437>.
- Winefordner, J.D., 2009. *Liquid Chromatography Times of Mass Spectrometry*. Wiley Inc Publication, New Jersey.
- Xu, X., Wang, B., Tang, H., Jin, Z., Mao, Y., Huang, T., 2020. Removal of phosphate from wastewater by modified bentonite entrapped in Ca-alginate beads. *J. Environ. Manage.* 260,. <https://doi.org/10.1016/j.jenvman.2020.110130> 110130.
- Zhang, T., Zhang, H., 2022. Microbial Consortia Are Needed to Degrade Soil Pollutants. *Microorganisms* 10, 261. <https://doi.org/10.3390/microorganisms10020261>.
- Zhang, Z., Xu, J., Yang, X., 2021. MXene / sodium alginate gel beads for adsorption of Methylene Blue. *Mater. Chem. Phys.* 260,. <https://doi.org/10.1016/j.matchemphys.2020.124123> 124123.
- Zytkiewicz, B.G., Sawicka, S., Karpinska, J., 2019. Removal of platinum and palladium from wastewater by means of biosorption on fungi *Aspergillus* sp. and yeast *Saccharomyces* sp. *Water* 11, 1522. <https://doi.org/10.3390/w11071522>.